



# Digital Mammography, Ultrasound and Magnetic Resonance Imaging Characteristics in Differential Diagnosis of Papillary Carcinoma Subtypes of the Breast and Diagnostic Challenges

İD Tuğba İlkem Kurtoğlu Özçağlayan<sup>1</sup>, İD Meltem Öznur<sup>2</sup>

<sup>1</sup>Department of Radiology, Liv Hospital Vadistanbul, İstanbul, Turkey

<sup>2</sup>Department of Pathology, Tekirdağ Namık Kemal University School of Medicine, Tekirdağ, Turkey

## ABSTRACT

**Objective:** We aimed to investigate mammography (MG), ultrasound (US), and magnetic resonance imaging (MRI) findings of papillary breast carcinoma subtypes and to compare the diagnostic features and performance of the imaging method in distinguishing subtypes.

**Materials and Methods:** Forty-two patients presenting with pathological diagnosis of 45 papillary carcinoma lesions, between 2014 and 2019, were included. Cases were assigned to five subgroups according to the latest World Health Organization (WHO) classification. The clinical characteristics (n = 45) and imaging features of each pathological subgroup were retrospectively related to imaging findings from US (n = 45), MG (n = 37), and breast MRI (n = 23), and further compared.

**Results:** The finding of a palpable mass in all subgroups was more common than nipple discharge on clinical breast evaluation, and no significant difference was found between the subgroups. Irregular shape on MG (10/12, 83.3%,  $p = 0.039$ ) and US (11/12, 91.7%,  $p = 0.039$ ) was found more frequently in invasive micropapillary carcinoma (IMPC) compared to other subgroups. Circumscribed margins (4/5, 80%,  $p = 0.002$ ) occurred more frequently in papillary ductal carcinoma *in situ* (pDCIS) and encapsulated papillary carcinoma (EPC) than in other subgroups (6/8, 75%,  $p = 0.002$ ). Lower apparent diffusion coefficient (ADC) values were found in solid papillary cancer (SPC) than in other subgroups ( $ADC = 0.35 \times 10^{-3}$ ,  $p = 0.017$ ).

**Conclusion:** Radiological findings of papillary carcinomas overlap with each other. US and MRI are complementary when revealing specific morphological characteristics.

**Keywords:** Breast; cancer; magnetic resonance imaging; mammography; ultrasound

**Cite this article as:** Kurtoğlu Özçağlayan Tİ, Öznur M. Digital Mammography, Ultrasound and Magnetic Resonance Imaging Characteristics in Differential Diagnosis of Papillary Carcinoma Subtypes of the Breast and Diagnostic Challenges. Eur J Breast Health 2022; 18(2): 172-181

## Key Points

- Due to their varying malignant potential, and nonspecific findings on imaging and histopathology, it is important to identify specific radiological findings in the differential diagnosis of papillary lesions.
- Ultrasound (US) and magnetic resonance imaging (MRI) were better at revealing the morphological characteristics of papillary lesions than mammography (MG). Furthermore, MRI was more useful than MG and US in showing the local spread of lesions and accompanying synchronous tumors.
- Both solid papillary carcinoma and encapsulated papillary carcinoma without invasive focus might be observed as oval or round well-circumscribed lesions on MG and can often be evaluated as BI-RADS 3 lesions
- Papillary neoplasms on MRI are similar to other invasive breast cancers in enhancement kinetics and diffusion restriction properties.

## Introduction

Papillary lesions of the breast are a group of proliferative diseases with solid components, typically cystic in nature and characterized by florid epithelial hyperplasia, originating from the ducto-lobular system (1, 2). Papillary carcinomas constitute less than 2% of all breast carcinomas (3) and the vast majority is seen in postmenopausal women (4). The intraductal papillary neoplasms of the breast include papilloma, papilloma with atypical ductal hyperplasia or ductal carcinoma *in situ* (DCIS), papillary DCIS (pDCIS), encapsulated papillary carcinoma (EPC), solid papillary carcinoma (SPC) and invasive papillary carcinoma (IPC) (5, 6). Invasive micropapillary carcinoma (IMPC) entity is listed under the invasive breast carcinoma category in the latest World Health Organization (WHO) classification of breast tumors (7).

Due to their varying malignant potential, and nonspecific findings on imaging and histopathology, papillary lesions present significant diagnostic and treatment challenges for radiologists, pathologists, and surgeons. The possibility of a high-risk lesion and neoplasia after excision of lesions shown to be benign papillomas by core biopsy has been demonstrated in previous studies (8). This situation has made it more important to reveal specific radiological findings in the differential diagnosis of papillary lesions.

There are publications about the contribution of imaging findings in the differentiation of benign and malignant papillary lesions (8, 9). However, there is a limited number of articles that examine all malignant papillary lesions subtypes and report their distinctive features from each other. In this large group of benign, *in-situ*, and invasive lesions, it is important to define the diagnostic radiological features of the lesions from each other, to indicate the correct surgical approach in the treatment of these lesions, and to prevent inadequate or excessive surgical treatments.

In this comprehensive study, we retrospectively examined the clinical and imaging findings of subtypes of malignant papillary lesions according to the current WHO classification. We aimed to investigate the differences between ultrasound (US), mammography (MG), and magnetic resonance imaging (MRI) findings in papillary breast cancers and to compare the advantages and disadvantages of imaging methods in distinguishing subtypes.

## Materials and Methods

### Patients and Histopathology

This study was conducted with the approval of the local ethics committee (approval number: 2019.119.07.15) dated 06/27/2019. Informed consent was obtained from all patients included in the study. Patients with papillary lesions diagnosed by histopathology at Tekirdağ Namık Kemal University School of Medicine Education and Research Hospital between 2014–2019 were obtained from the hospital patient data base management system. Hematoxylin&Eosin and Immunohistochemically stained slides of these patients were taken from the pathology archive and re-evaluated by a histopathologist with more than ten years experience. Case diagnosis was updated according to the latest WHO classification (WHO classification of tumors, 2019, 5<sup>th</sup> edition) (7). According to this classification, patients diagnosed with intraductal papilloma were excluded from the study. Patients with pDCIS, EPC, IPC, SPC (for both *in situ* and invasive), and IMPC under the heading of papillary neoplasms were included in the study. There were two separate (EPC and SPC) lesions in one

case. There were also three separate (one IMPC and two separate EPC) lesions in another case. There was co-existence of EPC and invasive ductal carcinoma (IDC) in two cases. As a result, 42 patients and 45 lesions with preoperative imaging findings were included in the study.

### Clinical Features

Patient demographic and clinical characteristics, such as age, lesion location, palpable lesion, and nipple discharge, were recorded. Lesions with a distance of less than 3 cm to the nipple were classified as central, and those with a distance of 3 cm or more were classified as peripheral. Lesion size was evaluated according to the largest diameter measured on MRI, mammography, or US images. Axillary lymph node involvement was recorded according to postoperative pathology results.

### Imaging Techniques

Thirty-seven out of 42 patients had MG, 42/42 had US, and 23/42 had MRI examinations, respectively. MG examinations were obtained using the Selenia™ Dimensions Mammography System (Hologic™, USA) device. MGs were examined in two standard projections, craniocaudal and medio lateral oblique. US was performed by the same radiologist in an unblinded setting with the Toshiba™ Applio™ XG device, using a 6–12 MHz linear transducer. All MRI examinations were obtained using a 1.5-T, whole-body, MRI scanner (BRIVO MR 355, GE™ Healthcare™, USA) device with an eight-channel breast coil.

With the examination performed in the prone position, the MRI protocol was as follows: Axial T2W fat-saturated image time of repetition (TR) 5,490 ms, time of echos (TE) 85 ms, slice thickness 5 mm, and matrix 320 x 256. T1W Spoiled Gradient Echo (SPGR) was also used with the settings: TR/TE: 4.8 ms/2.2 msn, slice thickness 2 mm, matrix 360 x 360 x 128. Gadoteric acid (Dotarem™, Guerbet™) was administered at a dose of 0.1 mmol/kg at a rate of 2 mL/sec, followed by administration of 20 mL/sec saline for 6 times for contrast-enhanced MRI images. The first acquisition started at 25 seconds after contrast injection. Imaging parameters of diffusion-weighted imaging (DWI) with  $b = 1,000 \text{ s/mm}^2$  value of the breast were TR/TE 6,050/84.3 ms, slice thickness/slice spacing was 5 mm/1 mm, field-of-view was 30 x 32 cm, and reconstruction matrix of 256 x 256.

### Imaging Interpretation

All radiological images were evaluated retrospectively by the same radiologist with ten years of experience. Imaging findings from US, MG, and MRI were evaluated using the latest atlas of the American College of Radiology Breast Imaging Reporting and Data System (ACR-BI-RADS 2013). On MG, the visibility of the lesion was evaluated initially. Breast composition BI-RADS final assessment categories were recorded. According to the categories in the ACR BI-RADS atlas, lesion characteristics (mass, asymmetry, calcification), shape of mass (oval, round, or irregular), margin of mass (circumscribed, obscured, microlobulated, indistinct, or spiculated), density of mass (compared to fat, low, equal, or high) and associated features (skin retraction, nipple retraction, skin thickness, or architectural distortion) were evaluated. Calcifications were evaluated according to morphology and distribution characteristics. US features were assessed for mass (shape, margin, orientation, echo pattern, or posterior features) and associated features (ductal changes, or vascularity).

MRI findings were examined in two groups, divided into those with mass enhancement and non-mass enhancement. Cases with both mass

lesions and non-mass enhancement were included in both categories. Non-mass enhancements were evaluated according to their distribution and enhancement pattern. Ductal ectasia was evaluated as ductal high signal intensities in precontrast T1W images on MRI examinations or dilated ductus in the US image. The kinetic enhancement curve was evaluated in dynamic contrast series. Apparent diffusion coefficient (ADC) values were measured and recorded in DWI sequences.

**Statistical Analysis**

Data analysis was performed using IBM SPSS, version 17.0 (IBM Inc., Armonk, NY, USA). Shapiro–Wilk test was used to determine whether the distributions of continuous variables were normal or not. The assumption of homogeneity of variances was examined by the Levene test. Descriptive statistics were expressed as mean ± standard deviation, median (25<sup>th</sup>–75<sup>th</sup>) percentiles or the number of cases, and

(%), where appropriate. While the differences in BI-RADS, maximum lesion size, and DWI values among subgroups were compared by using Kruskal–Wallis test, a one-way ANOVA test was applied for the comparison of age levels. A chi-square test was used for categorical variables. If the expected number of categorical variables in any group was less than 5, the Fischer test *p*-value was accepted. *p*<0.05 was considered statistically significant.

**Results**

Two of the patients were men and 40 were women. One of the male cases was diagnosed with pDCIS and the other with EPC. Descriptive characteristics and clinical findings of the cases are shown in Table 1. There was no statistical difference in the papillary cancer subgroups in terms of previous history of breast cancer, BI-RADS classifications of

Table 1. Descriptive characteristics of study population

	Papillary DCIS (n = 5)	Encapsulated (cystic) papillary ca (n = 8)	Solid papillary (n = 7)	Invasive papillary (n = 13)	Invasive micropapillary (n = 12)	<i>p</i> -value
<b>Mean age (years)</b>	62.2±19.9	62.9±10.6	56.6±10.3	62.7±13.4	60.4±8.2	0.835†
<b>Gender</b>						
<b>Male</b>	1 (20.0%)	1 (12.5%)	0 (0.0%)	0 (0.0%)	0 (0.0%)	0.202‡
<b>Female</b>	4 (80.0%)	7 (87.5%)	7 (100.0%)	13 (100.0%)	12 (100.0%)	
<b>Previous breast ca</b>	1 (20.0%)	3 (37.5%)	2 (28.6%)	1 (7.7%)	0 (0.0%)	0.138‡
<b>Palpation</b>	5 (100.0%)	6 (75.0%)	7 (100.0%)	11 (84.6%)	7 (58.3%)	0.146‡
<b>Nipple discharge</b>	1 (20.0%)	4 (50.0%) <sup>a</sup>	0 (0.0%)	1 (7.7%) <sup>a</sup>	1 (8.3%)	<b>0.044‡</b>
<b>BI-RADS</b>						
0	0 (0.0%)	3 (37.5%)	0 (0.0%)	0 (0.0%)	0 (0.0%)	0.217¶
3	1 (20.0%)	0 (0.0%)	0 (0.0%)	0 (0.0%)	0 (0.0%)	
4a	1 (20.0%)	0 (0.0%)	0 (0.0%)	3 (23.1%)	1 (8.3%)	
4b	0 (0.0%)	0 (0.0%)	0 (0.0%)	2 (15.4%)	0 (0.0%)	
4c	1 (20.0%)	1 (12.5%)	2 (28.6%)	1 (7.7%)	1 (8.3%)	
5	2 (40.0%)	4 (50.0%)	5 (71.4%)	7 (53.8%)	10 (83.3%)	
<b>Breast composition</b>						
A	0 (0.0%)	2 (28.6%)	1 (14.3%)	2 (15.4%)	0 (0.0%)	0.352‡
B	2 (50.0%)	3 (42.9%)	5 (71.4%)	10 (76.9%)	9 (75.0%)	
C	2 (50.0%)	1 (14.3%)	1 (14.3%)	1 (7.7%)	3 (25.0%)	
D	0 (0.0%)	1 (14.3%)	0 (0.0%)	0 (0.0%)	0 (0.0%)	
<b>Lesion side</b>						
Left	3 (60.0%)	5 (62.5%)	3 (42.9%)	6 (46.2%)	6 (50.0%)	0.939‡
Right	2 (40.0%)	3 (37.5%)	4 (57.1%)	7 (53.8%)	6 (50.0%)	
<b>Location</b>						
Central	3 (60.0%)	6 (75.0%)	5 (71.4%)	4 (30.8%)	6 (50.0%)	0.285‡
Peripheral	2 (40.0%)	2 (25.0%)	2 (28.6%)	9 (69.2%)	6 (50.0%)	
Maximum diameter	52.0 (18.5–70.0)	29.5 (19.0–34.7)	22.0 (17.0–26.0)	23.0 (14.5–37.5)	17.5 (10.7–23.5)	0.160¶
Axillary lymphadenopathy	-	<b>3 (75.0%)</b>	<b>1 (16.7%)</b>	<b>3 (60.0%)</b>	<b>3 (50.0%)</b>	<b>0.521†</b>

Significant values are shown in bold.

Data are shown as mean ± SD, median (25<sup>th</sup>–75<sup>th</sup> percentiles) and n (%). †One-Way ANOVA, ‡Fisher-Freeman Holton test, ¶Kruskal-Wallis test, <sup>a</sup>: Encapsulated papillary Ca vs. invasive papillary Ca (p = 0.047).

BI-RADS: Breast Imaging Reporting and Data System; DCIS: ductal carcinoma *in situ*; ca: carcinoma; n: number; SD: standard deviation

lesions, breast composition, lesion side, lesion location, the maximum diameter of lesions, or axillary lymph node involvement (Table 1). Although the finding of a palpable mass in all subgroups was more common than nipple discharge on clinical breast evaluation, no significant difference was found between the subgroups ( $p > 0.05$ ). There was a significant difference between the subgroups in terms of nipple discharge ( $p = 0.044$ ) with the rate of nipple discharge being higher in the EPC subgroup (4/8, 50%) compared to the IPC subgroup (1/13, 7.7%,  $p = 0.047$ ) (Table 1) although it is less common clinical finding among the subgroups.

### Imaging Characteristics

In the study subgroup, lesions were detected in four of five cases in pDCIS, seven of eight cases in EPC, six of seven cases in SPC, eight of 13 cases in IPC, and 12 of 12 cases in IMPC on MG imaging. Lesions were occult in eight cases on MG imaging. When MG characteristics of the subgroups were compared with each other, lesions in the IMPC subgroup were frequently observed as irregularly shaped (Figure 1), while those in EPC subgroup were often found to be round or oval-shaped. There was a significant difference in IMPC subgroup in terms of frequency of occurrence of irregular shape ( $p = 0.039$ ), and the rate of irregularities in IMPC subgroup was higher than in EPC subgroup ( $p = 0.006$ ). There was a significant difference between the subgroups in terms of the frequency of margins being circumscribed or non-circumscribed ( $p = 0.017$ ). The circumscribed rate was higher in pDCIS subgroup compared to that of the SPC and IMPC subgroups ( $p = 0.033$  and  $p = 0.027$ , respectively). The ratio of circumscribed margin in the IMPC subgroup was also statistically significantly lower than in the EPC subgroup ( $p = 0.038$ ). There was no statistical difference between subgroups in terms of calcification. Calcification was similarly observed in SPC (33.3%) and IMPC (33.3%), and it was amorphous or finely pleomorphic. There was no statistical difference between the subgroups for the presence of skin retraction, nipple retraction, architectural distortion, and other characteristics examined ( $p > 0.05$ ) (Table 2).

In comparison to their ultrasonographic features, there was a significant difference between the subgroups in terms of irregular shape ( $p = 0.039$ ) with the rate of occurrence of irregularities in the IMPC subgroup being higher than in the EPC and SPC subgroups ( $p = 0.004$  and  $p = 0.038$ , respectively). There was also a difference between the subgroups in respect of circumscribed margins ( $p = 0.002$ ). The circumscribed margin rate was higher in the pDCIS subgroup compared to SPC and IMPC subgroups ( $p = 0.010$  and  $p = 0.019$ , respectively). The circumscribed margin rate was significantly higher in the EPC subgroup than in the SPC and IMPC subgroups ( $p = 0.007$  and  $p = 0.028$ , respectively) (Figure 2). A significant difference was also found between the subgroups in terms of the ratio of cystic/solid echopattern ( $p = 0.006$ ), with this ratio being higher in the pDCIS and EPC subgroups compared to the SPC subgroup ( $p = 0.031$  and  $p = 0.006$ , respectively) (Figure 3). There was no difference between subgroups as to other characteristics examined ( $p > 0.05$ ) (Table 3).

No statistical difference was observed for subgroup comparisons in respect of mass enhancement and non-mass enhancement ( $p = 0.682$  and  $p = 0.964$ ) on MRI. The distributions of non-enhancing findings, axillary lymphadenopathy, and kinetic curve assessment findings of the subgroups were similar ( $p > 0.05$ ). All lesions were slightly hyperintense on DWI, and ADC values ranged from  $0.1 \times 10^{-3} \text{ mm}^2/\text{s}$  to  $1.5 \times 10^{-3} \text{ mm}^2/\text{s}$ . There was a statistically significant difference in ADC levels

between subgroups ( $p = 0.017$ ), which was lower in the SPC subgroup compared to the IPC subgroup ( $p = 0.036$ ) (Table 4).

### Discussion and Conclusion

Our study demonstrated that there was no distinctive radiological imaging feature that distinguishes subgroups of papillary breast carcinomas, and papillary carcinomas may have imaging features similar to other invasive breast tumors. Papillary lesions should be

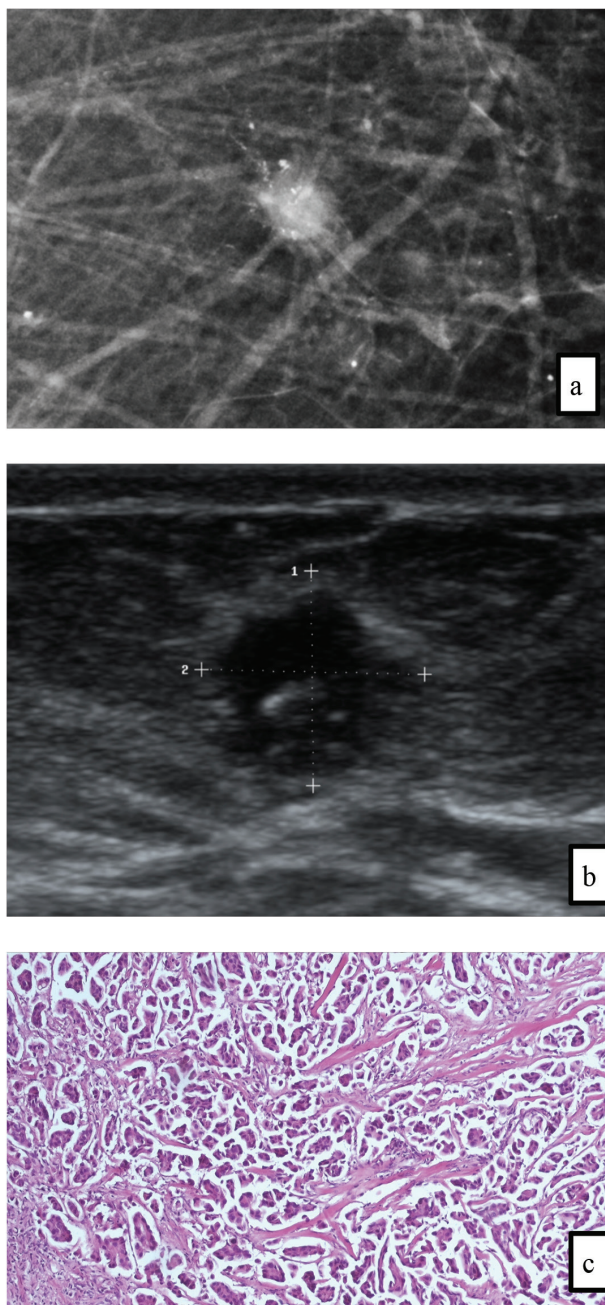


**Figure 1.** Invasive micropapillary carcinoma in 65-year old woman who underwent MG screening. **a)** A magnified cranio-caudal mammogram shows the irregular, high density mass with spiculated margins and pleomorphic microcalcifications. **b)** Gray scale US image shows the same lesion as hypoechoic mass with spiculated margins in the low inner quadrant. **c)** Photomicrography shows clusters of tumor cells in a micropapillary arrangement that appears to be within empty stromal spaces (H&E stain, x200).

MG: mammography; US: ultrasonography; H&E: hematoxylin & eosin

Table 2. Mammographic characteristics of study population

	Papillary DCIS (n = 4)	Encapsulated (cystic) papillary ca (n = 7)	Solid papillary (n = 6)	Invasive papillary (n = 8)	Invasive micropapillary (n = 12)	p-value
<b>Shape of mass</b>						
Oval	2 (50.0%)	4 (57.1%)	1 (16.7%)	5 (62.5%)	2 (16.7%)	0.155†
Round	0 (0.0%)	2 (28.6%)	1 (16.7%)	0 (0.0%)	0 (0.0%)	0.170†
Irregular	2 (50.0%)	1 (14.3%) <sup>a</sup>	4 (66.7%)	3 (37.5%)	10 (83.3%) <sup>a</sup>	<b>0.039†</b>
<b>Margin of mass</b>						
Circumscribed	3 (75.0%) <sup>b,c</sup>	4 (57.1%) <sup>a</sup>	0 (0.0%) <sup>b</sup>	3 (37.5%)	1 (8.3%) <sup>a,c</sup>	
Not circumscribed	1 (25.0%) <sup>b,c</sup>	3 (42.9%) <sup>a</sup>	6 (100.0%) <sup>b</sup>	5 (62.5%)	11 (91.7%) <sup>a,c</sup>	<b>0.017†</b>
<b>Density of mass</b>						
Equal	1 (25.0%)	2 (28.6%)	4 (66.7%)	4 (57.1%)	4 (33.3%)	
High	3 (75.0%)	5 (71.4%)	2 (33.3%)	3 (42.9%)	8 (66.7%)	0.524†
Asymmetry	0 (0.0%)	0 (0.0%)	0 (0.0%)	0 (0.0%)	0 (0.0%)	-
<b>Calcifications</b>						
Morphology	0 (0.0%)	0 (0.0%)	2 (33.3%)	0 (0.0%)	4 (33.3%)	
			2 amorphous	0 (0.0%)	2 amorphous	
			2 (33.3%)		2 fine pleomorphic	0.104†
					4 (33.3%)	
Distribution	0 (0.0%)	0 (0.0%)	2 grouped	0 (0.0%)	4 grouped	0.104†
<b>Associated features</b>						
Skin retraction	1 (25.0)	0 (0.0%)	3 (50.0%)	0 (0.0%)	1 (9.1%)	
Nipple retraction	2 (50.0%)	1 (14.3%)	0 (0.0%)	0 (0.0%)	0 (0.0%)	
Skin thickening	1 (25.0%)	1 (14.3%)	3 (50.0%)	1 (14.3%)	1 (9.1%)	0.573†
Architectural distortion	1 (25.0%)	2 (28.6%)	1 (16.7%)	0 (0.0%)	0 (0.0%)	

Significant values are shown in bold.

Data are shown as n (%). †Fisher Freeman Holton test, <sup>a</sup>: Encapsulated papillary ca vs. invasive micropapillary ca (p<0.05), <sup>b</sup>: Papillary DCIS vs. solid papillary (p = 0.033), <sup>c</sup>: Papillary DCIS vs. invasive micropapillary (p = 0.027).

DCIS: ductal carcinoma in situ; ca: carcinoma; n: number

considered in the differential diagnosis if lesions show a morphological relation to duct structures and/or present as complex cystic and solid findings. Both US and MRI were better for revealing the morphological characteristics of papillary lesions than MG, and MRI was more useful than MG and US in showing the local spread of lesions and accompanying synchronous tumors.

Imaging findings of papillary lesions of the breast with benign or malignant breast lesions are various and can be confused radiologically. They can be seen as mass formation with smooth or irregular borders, as well as non-mass lesions with indistinct borders. Since lesions originate from ductal structures, their relationship with ductal structures may not always be demonstrated by imaging methods. Therefore, papillary lesions of the breast can be classified into different categories, ranging from BI-RADS 3 to BI-RADS 5.

In our study, all cases in subgroups occurred most frequently in the sixth decade. Among all subgroups, the youngest patient was diagnosed as IPC at the age of 34, and the oldest patient was in SPC (*in situ*) subgroup at the age of 90. There are several studies in the literature reporting that SPC maybe seen in the young patient group, and a few publications are reporting that SPC might also be seen in patients

in their 20s (10, 11). There have been rare publications that report papillary lesions in male patients, such as a study done by Zhong et al. (12), which reported 117 male cases in a period of 19 years. In our study, we had two male cases, one pDCIS, and one EPC.

Papillary lesions of the breast present as clinically palpable mass or nipple discharge. In our study, nipple discharge was most frequently observed in the EPC subgroup (50%). Nipple discharge has been seen less frequently with a rate of 0%–50% among all subgroups in our study. Bloody nipple discharge was reported in at least one-third of EPCs in the literature (13, 14). Although serous or bloody nipple discharge may occur in papillary carcinomas, in our cohort it was not a very common clinical finding. On the other hand, mass lesions palpated by clinical examination are more common in all subgroups and it was seen in 58%–100% of all groups in our study. Palpable mass findings were mostly observed in the SPC and the pDCIS subgroups. A clinically palpable mass lesion is usually related to the tumor diameter. The subgroup with the highest mean tumor diameter was pDCIS, and the subgroup with the lowest was the IMPC in our study. IMPC is a more aggressive tumor and may be associated with lymph node involvement, even in a smaller size, due to its lymphoproliferative nature. Lymph node involvement is frequently

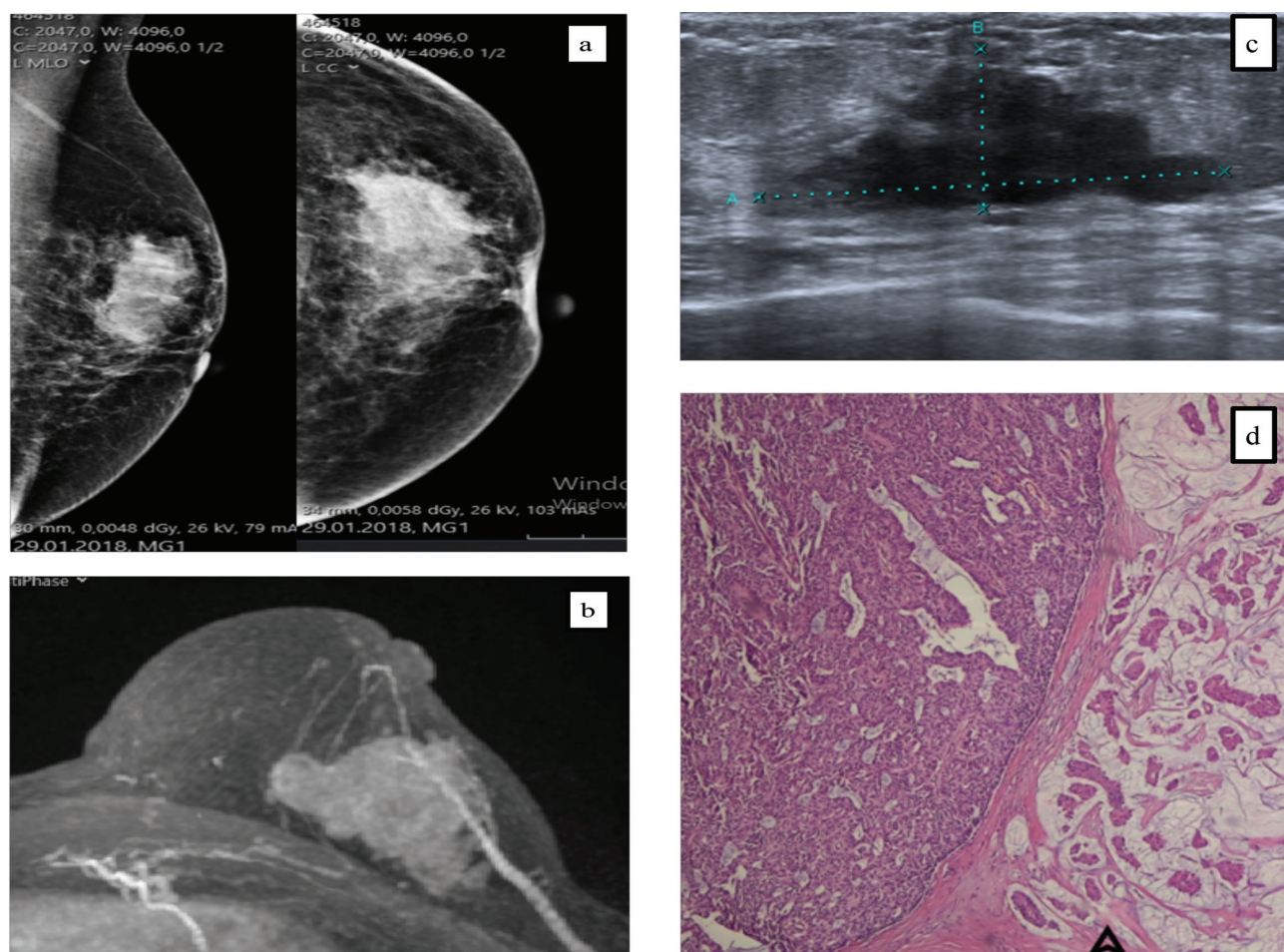


**Figure 2.** Solid papillary carcinoma in 65-year old woman who underwent MG screening. **a)** Mediolateral oblique and cranio-caudal MG shows irregular shaped dense mass in upper outer quadrant. **b)** Axial T1W SPGR contrast-enhanced 3D MRI image shows an irregular circumscribed mass with heterogenous enhancement. **c)** US image shows a hypoechoic mass with irregular borders. **d)** Photomicrograph shows the solid papillary carcinoma with a well-defined solid growth pattern, fibrovascular cores and monotonous population of ovoid to spindle-shaped epithelial cells with an invasive carcinoma component (arrowhead) (H&E stain, x200).

MG: mammography; MRI: magnetic resonance imaging; SPGR: spoiled gradient echo; US: ultrasonography; H&E: hematoxylin & eosin

present due to its significant lymphotrophic character at the time of initial diagnosis of IMPCs (13, 15). In many studies, axillary lymph node involvement has been reported, at rates ranging from 69%–95% (16, 17). Axillary lymph node involvement was present in only 50% of IMPC cases in our study.

In our study, locations of lesions were usually central, and no statistical difference was shown between subgroups, although the rate of central location was the highest in the EPC subgroup (75%). In parallel with our findings, a few publications showed that EPC was frequently centrally located and presented with a palpable mass in the retroareolar region (5, 18). We found that the IPC subgroup was the most peripheral subgroup (69.2%) among all subgroups and presented with a palpable mass. In the literature, half of the masses were reported to be centrally located and presented with a nipple discharge (13).

It is very difficult to differentiate papillary tumors by imaging methods, especially by MG. The percentage of occult lesions was 18% in MG. With a rate of 62% the subgroup with the highest rate of occult lesions was IPC. This finding may be explained because 21% of the study group had type C and type D

breast density, and breast tissue superimposed over the lesions. Another reason was the difficulty in determining multiple foci with a segmental distribution using MG, which does not establish mass formation, especially in IPC cases. Our study showed that papillary carcinomas can be observed on MG as either circumscribed lesions with oval or lobulated contours or asymmetric densities. Although they are frequently observed as well-circumscribed masses, as reported in the literature, they may have indistinct margins. Microcalcifications were often amorphous and finely pleomorphic calcifications. There was no microcalcification in the pDCIS subgroup. However, linear, granular, or fixed calcification can be seen in pDCIS. We did not observe calcifications as an associated feature in EPC. Accompanying microcalcification in EPC has been rarely reported in the literature (19). Concomitant microcalcification on MG was rarely reported in the literature in SPC cases (20, 21), and 33.32% of SPC in our study were accompanied by amorphous calcifications. We found no mammographic microcalcification of IPC cases. However, Ciurea et al. (18) reported IPCs as round or lobulated masses, often associated with mammographic calcification. IMPC is a clinically aggressive variant of invasive carcinomas. IMPCs are irregular, spiculated, or indistinct, high-density masses on MG (15, 22). In our study,

IMPC was the most common mammographic mass formation and concomitant microcalcification was observed in 33.3% of the cases. In the literature, concomitant microcalcification has been reported in 48%–68% of IMPC cases (15, 22, 23). According to our findings, although both SPC and IMPCs were most commonly accompanied

by microcalcification of the subgroups, no difference was found when compared with other subgroups. Papillary cancers often have similar mammographic features to other invasive breast tumors. Our study also showed that SPC and EPC without invasive focus might be observed as oval or round, well-circumscribed lesions on MG and can often be evaluated as BI-RADS 3 lesions. These oval, smooth-contoured lesions encountered in the sixth and seventh decades are observed to be higher density than the breast parenchyma and if they are growing during follow-up, they may have malignant character. For the differential diagnosis of papillary neoplasm, it may be useful to perform additional imaging modalities, such as US or MRI, in order to better reveal the morphological features.

US is a very useful tool in the diagnosis of papillary lesions. In the further evaluation of a mass detected on MG, sonographic demonstration of cystic lesions with solid, or solid components associated with ductal structures, should bring to mind papillary lesions, and it is more useful than MG. However, the relation of papillary lesions originating from peripheral ducts with ductal structures may not always be demonstrated. It may appear similar to other invasive breast tumors, as in the examples of IPC and IMPC. EPCs have been ultrasonographically described in some previous studies as complex, cystic mass lesions with solid papillary projection originating from the cyst wall (24, 25). The typical complex, cystic appearance was present in 50% of our EPC cases. As stated in the literature, this typical appearance described on US and MRI examinations should bring EPC to mind in the differential diagnosis. However, it has been reported in the literature that this appearance may be similar to benign lesions, such as well-defined fibroadenoma and phyllodes tumor, as well as malignant lesions, including medullary or mucinous carcinoma (26). For this reason, it should be kept in mind that EPC can also appear as hypoechoic solid lesions. The increase in size and morphological changes in follow-up examinations, accompanying ductal extension and ductal dilatation should be considered for the possibility of malignancy in these lesions. pDCIS was observed as a complex, cystic-solid lesion in 40% of our cases. The imaging findings of SPC cases are also quite variable, and it has been reported sonographically as multiple nodules accompanied by ductal ectasia, well-circumscribed, complex, cystic lesion, and homogeneous solid lesions (10, 27, 28). In our study, SPC was observed as round, well-demarcated, or irregularly shaped lesions with microlobulated or spiculated margins. According to our experience, it can be seen as irregularly shaped of microlobulated or spiculated solid lesions, especially in subtypes with invasive components. In these cases, biopsy should be performed with the modality in which the lesion is best seen. In cases accompanied by calcifications, sampling calcifications with mammography would be an appropriate approach. In lesions with cystic and solid components, a cut biopsy can be performed from the solid component after aspiration of the cyst content. Sometimes, repeat biopsy may be necessary if the pathology is not consistent with imaging findings. At this stage, preferring biopsy methods where more tissue can be sampled, or excisional biopsy, will be a more appropriate approach, especially in papillary carcinoma cases.

MRI features of papillary neoplasms vary according to their subtypes. There are different imaging features of subgroups in the MRI range from mass to non-mass enhancement in dynamic contrast-enhanced series. The majority of our cases showed mass enhancement. While all of the SPCs and EPCs showed mass enhancement, pDCIS, SPC, and IMPC cases showed both mass and non-mass enhancement. Similar to US, MRI is valuable in the morphological evaluation of papillary

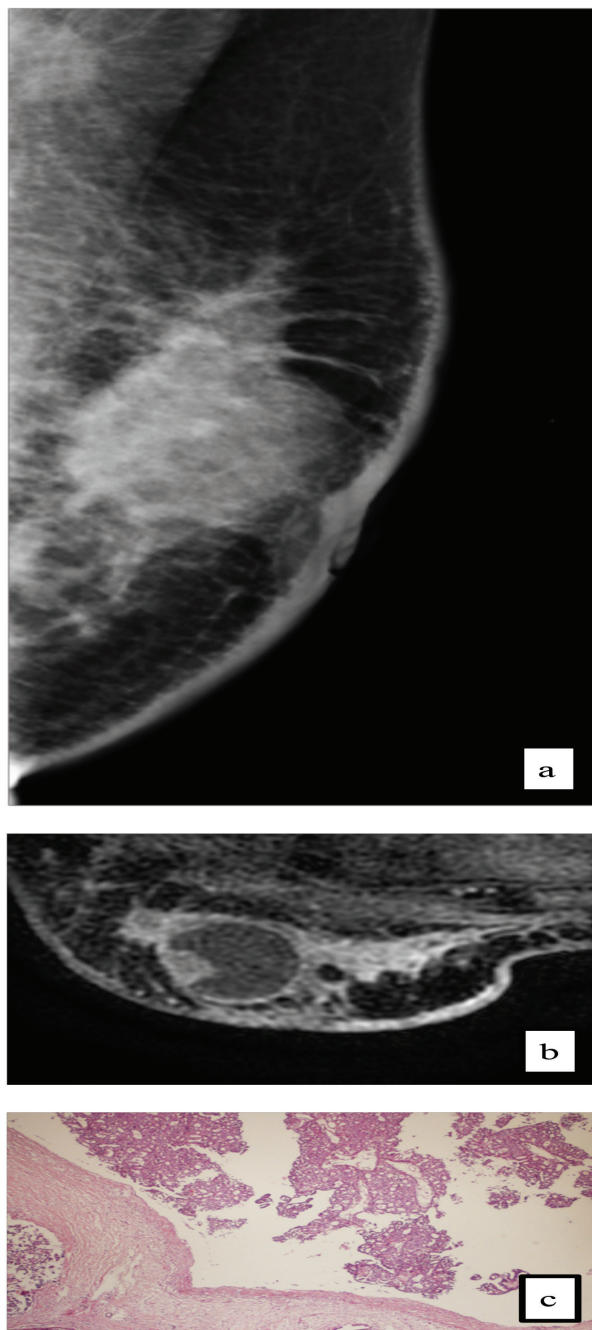


**Figure 3.** Encapsulated papillary carcinoma in a 50-year-old woman who presented with palpable lump. **a)** Mediolateral oblique mammogram shows the spiculated lesion with high density in the retroareolar location and associated axillary lymphadenopathy. **b)** Axial T1W contrast-enhanced MRI shows the complex cystic lesion with mural based nodule associated with invasive component at the posterolateral aspect of the lesion. **c)** Photomicrography shows the papillary proliferation, which consists of uniform cells surrounded by a fibrous capsule and does not contain myoepithelial cells (H&E stain, x100).

Table 3. Ultrasound characteristics of study population

	Papillary DCIS (n = 5)	Encapsulated (cystic) papillary ca (n = 8)	Solid papillary (n = 7)	Invasive papillary (n = 13)	Invasive micropapillary (n = 12)	p-value
<b>Shape</b>						
Oval	2 (40.0%)	3 (37.5%)	2 (28.6%)	6 (46.2%)	1 (8.3%)	0.348†
Round	0 (0.0%)	3 (37.5%)	2 (28.6%)	2 (15.4%)	0 (0.0%)	0.123†
Irregular	3 (60.0%)	2 (25.0%) <sup>a</sup>	3 (42.9%) <sup>b</sup>	7 (53.8%)	11 (91.7%) <sup>a,b</sup>	<b>0.039†</b>
<b>Margin</b>						
Circumscribed	4 (80.0%) <sup>c,d</sup>	6 (75.0%) <sup>a,e</sup>	0 (0.0%) <sup>c,e</sup>	4 (30.8%)	2 (16.7%) <sup>a,d</sup>	<b>0.002†</b>
Not circumscribed	1 (20.0%) <sup>c,d</sup>	2 (25.0%) <sup>a,e</sup>	7 (100.0%) <sup>c,e</sup>	9 (69.2%)	10 (83.3%) <sup>a,d</sup>	
<b>Orientation</b>						
Parallel	3 (60.0%)	4 (50.0%)	5 (71.4%)	9 (69.2%)	2 (16.7%)	0.068†
Not parallel	2 (40.0%)	4 (50.0%)	2 (28.6%)	4 (30.8%)	10 (83.3%)	
<b>Echo pattern</b>						
Isoechoic	0 (0.0%)	0 (0.0%)	0 (0.0%)	0 (0.0%)	0 (0.0%)	
Hypoechoic	3 (60.0%)	4 (50.0%)	7 (100.0%)	12 (92.3%) <sup>f</sup>	12 (100.0%) <sup>a</sup>	<b>0.006†</b>
Complex cystic/solid	2 (40.0%)	4 (50.0%) <sup>a,f</sup>	0 (0.0%)	1 (7.7%)	0 (0.0%)	
<b>Posterior features</b>						
No features	3 (60.0%)	6 (75.0%)	2 (28.6%)	8 (61.5%)	10 (83.3%)	
Posterior	2 (40.0%)	2 (25.0%)	5 (71.4%)	3 (23.0%)	2 (16.6%)	
Enhancement	0 (0.0%)	2 (25.0%)	0 (0.0%)	0 (0.0%)	0 (0.0%)	0.193†
Shadowing	2 (40.0%)	2 (25.0%)	2 (28.6%)	10 (77.0%)	10 (83.4%)	
Combined	1 (20.0%)	2 (25.0%)	0 (0.0%)	0 (0.0%)	0 (0.0%)	
<b>Associated features</b>						
Duct changes	1 (20.0%)	0 (0.0%)	2 (28.5%)	2 (15.4%)	2 (16.6%)	0.149†
Vascularity	2 (40.0%)	2 (25.0%)	5 (71.4%)	5 (38.4%)	4 (33.2%)	

Significant values are shown in bold.

Data are shown as n (%). †Fisher Freeman Holton test, <sup>a</sup>: Encapsulated papillary ca vs. invasive micropapillary ( $p < 0.05$ ), <sup>b</sup>: Solid papillary vs. invasive micropapillary ( $p = 0.038$ ), <sup>c</sup>: Papillary DCIS vs. solid papillary ( $p = 0.010$ ), <sup>d</sup>: Papillary DCIS vs. invasive micropapillary ( $p = 0.028$ ), <sup>e</sup>: Encapsulated papillary ca vs. solid papillary ( $p = 0.007$ ), <sup>f</sup>: Encapsulated papillary ca vs. invasive papillary ( $p = 0.047$ ).

DCIS: ductal carcinoma *in situ*; ca: carcinoma; n: number

lesions and demonstrates their relationship with ductal structures. MRI has been useful in determining lesions, including pDCIS with a non-mass contrast enhancement pattern, that are mammographically occult and observed with indeterminate borders on US, and it shows typical morphological features of EPC cases with intracystic solid components. Besides morphological appearance, MRI plays a valuable role, especially in preoperative mapping, evaluation of local extension, and showing accompanying DCIS and invasive foci (29, 30). In one case from our study, there was co-existence of EPC and SPC and in one further case there were three separate lesions, one IMPC, and two separate EPC, while in two cases there was an association of EPC-invasive ductal carcinoma (IDC). We suggest that EPCs can be divided into *in situ* and invasive subgroups, like SPC.

Papillary neoplasms are similar to other invasive breast cancers in terms of enhancement kinetics and diffusion restriction properties. Similar to the literature, we found that papillary lesions often showed rapid enhancement kinetics in the early phase and wash out or plateau in the middle and late phases on dynamic contrast-enhanced imaging. There

was no difference between subgroups in the case of contrast kinetics and diffusion features.

The limitations of our study were its retrospective design, an insufficient number of study patients which reflects the rarity of this uncommon tumor and heterogeneous subgroups, as well as lack of interobserver and intraobserver reliability testing.

In conclusion, subgroups of papillary carcinomas are extremely rare breast entities, presenting with radiological findings overlapping each other. US and MRI are more useful than mammography in revealing the relationship between the lesions and ductal structures. MRI is one step ahead of the other modalities in showing papillary lesions, and it is the most useful modality in preoperative evaluation. Although imaging findings do not reveal clear data in distinguishing these lesions, radiologists should carefully assess the clues that suggest papillary lesions in imaging findings and consider papillary lesions and subtypes in the differential diagnosis.



Table 4. Magnetic resonance characteristics of study population

	Papillary DCIS (n = 2)	Encapsulated (cystic) papillary ca (n = 4)	Solid papillary (n = 6)	Invasive papillary (n = 5)	Invasive micropapillary (n = 6)	p-value
<b>MASS</b>	<b>1 (50.0%)</b>	<b>4 (100.0%)</b>	<b>5 (83.3%)</b>	<b>5 (100.0%)</b>	<b>5 (83.3%)</b>	
<b>Shape</b>						
Oval	-	1 (25.0%)	-	1 (20.0%)	-	
Round	-	3 (75.0%)	2 (33.3%)	1 (20.0%)	1 (16.6%)	
Irregular	1 (50.0%)	-	3 (50.0%)	3 (60.0%)	4 (66.6%)	
<b>Margin</b>						
Circumcribed	1 (50.0%)	4 (100.0%)	-	1 (20.0%)	-	
Non circumcribed	-	-	5 (83.3%)	4 (80.0%)	5 (83.3%)	
<b>Internal enhancement</b>						<b>0.682†</b>
Homogenous	-	-	1 (16.6%)	-	1 (16.6%)	
Heterogenous	1 (50.0%)	1 (25.0%)	4 (66.6%)	5 (100.0%)	4 (66.6%)	
Rim enhancement	-	3 (75.0%)	-	-	-	
<b>Non MASS distribution</b>	<b>1 (50.0%)</b>	<b>2 (50.0%)**</b>	<b>2(33.3%)**</b>	<b>3 (60.0%)**</b>	<b>3 (50.0%)**</b>	
Segmental	1 (50.0%)	-	-	-	1 (16.6%)	
Regional	-	-	1 (16.6%)	-	-	
<b>Internal enhancement</b>						<b>0.964†</b>
Homogenous	-	-	1 (16.6%)	-	1 (16.6%)	
Heterogenous	1 (50.0%)	-	5 (83.3%)	-	-	
<b>Non enhancing findings</b>	<b>0 (0.0%)</b>	<b>1 (25.0%)</b>	<b>3 (50.0%)</b>	<b>3 (60.0%)</b>	<b>0 (0.0%)</b>	<b>0.175†</b>
<b>Kinetic curve assessment</b>						
Persistent	-	-	-	-	-	
Plateau	1 (50.0%)	3 (75.0%)	3 (50.0%)	4 (80.0%)	5 (83.3%)	<b>0.796†</b>
Washout	1 (50.0%)	1 (25.0%)	3 (50.0%)	1 (20.0%)	1 (16.7%)	
<b>DWI x 10<sup>-3</sup></b>	<b>1.35</b> <b>(1.30–1.40)</b>	<b>1.00</b> <b>(0.37–1.17)</b>	<b>0.35</b> <b>(0.10–0.90)<sup>a</sup></b>	<b>1.10</b> <b>(1.10–1.50)<sup>a</sup></b>	<b>1.20</b> <b>(0.90–1.50)</b>	<b>0.017‡</b>

Significant values are shown in bold.

Data are shown as median (25<sup>th</sup>-75<sup>th</sup> percentiles) and n (%). †Fisher Freeman Holton test, ‡Kruskal-Wallis test, <sup>a</sup>:Solid papillary vs invasive papillary (p = 0.036).

\*\* 2 cases in EPC subgroup, 1 case in SPC subgroup, 3 cases in IPC subgroup, 2 cases in IMPC subgroup showed both mass and non-mass enhancement.

DCIS: ductal carcinoma *in situ*; ca: carcinoma; EPC: encapsulated papillary carcinoma; IPC: invasive papillary carcinoma; DWI: diffusion-weighted imaging; n: number

**Acknowledgments**

The authors would like to thank Ömer Özçağlayan M.D., Assoc. Prof. Dr. and Sibel Özkan Gürdal M.D., Prof. Dr. for clinical and general support during this project.

**Ethics Committee Approval:** This study was approved by Tekirdağ Namık Kemal University Medical School Ethics Committee with “2019.119.07.15” approval number on 06.27.2019.

**Informed Consent:** Informed consent was obtained from all patients included in the study.

**Conflict of Interest:** All authors declare that there is no conflict of interest regarding this manuscript.

**Funding:** All authors declare that no funding was received for this study.

**Authorship Contributions**

Surgical and Medical Practices: T.İ.K.Ö., M.Ö.; Concept: T.İ.K.Ö., M.Ö.; Design: T.İ.K.Ö., M.Ö.; Data Collection and/or Processing: T.İ.K.Ö., M.Ö.; Analysis and/or Interpretation: T.İ.K.Ö.; Literature Search: M.Ö.; Writing: T.İ.K.Ö.

**Conflict of Interest:** No conflict of interest was declared by the authors.

**Financial Disclosure:** The authors declared that this study received no financial support.

## References

- O'Malley FP, Visscher D, MacGrogan G, Tan PH, Ichihara S. Intraductal papilloma. In: Lakhani S, Ellis I, Schnitt SJ, Tan PH, van de Vijver MJ, editors. WHO Classification of Tumours of the Breast. 4th ed. Lyon: IARC Press; 2012. p. 100-2. [\[Crossref\]](#)
- Tan PH, Schnitt SJ, van de Vijver MJ, Ellis IO, Lakhani SR. Papillary and neuroendocrine breast lesions: the WHO stance. *Histopathology* 2015; 66: 761-770. (PMID: 24845113) [\[Crossref\]](#)
- Mulligan AM, O'Malley FP. Papillary lesions of the breast: a review. *Adv Anat Pathol* 2007; 14: 108-119. (PMID: 17471117) [\[Crossref\]](#)
- Liberman L, Feng TL, Susnik B. Case 35: Intracystic papillary carcinoma with invasion. *Radiology* 2001; 219: 781-784. (PMID:11376269) [\[Crossref\]](#)
- Broggi E, Horii R, Mac Grogan G, et al. Papillary Neoplasms. Breast Tumours. WHO Classification of Tumours, 5th Edition, Volume 2 . WHO Classification of Tumours Editorial Board International Agency for Research on Cancer: Lyon; 2019. p. 49-67. [\[Crossref\]](#)
- Tan PH, Ellis I, Allison K, Brogi E, Fox SB, Lakhani S, et al. The 2019 World Health Organization classification of tumours of the breast. *Histopathology* 2020; 77: 181-185. (PMID: 32056259) [\[Crossref\]](#)
- Marchio C, Horlings HM, Vincent-Salomon A. Invasive Breast Carcinoma. Breast Tumours. WHO Classification of Tumours, 5th Edition, Volume 2 . WHO Classification of Tumours Editorial Board International Agency for Research on Cancer: Lyon; 2019. p. 128-130. [\[Crossref\]](#)
- Jagmohan P, Pool FJ, Putti TC, Wong J. Papillary lesions of the breast: imaging findings and diagnostic challenges. *Diagn Interv Radiol* 2013; 19: 471-478. (PMID: 23996839) [\[Crossref\]](#)
- Eiada R, Chong J, Kulkarni S, Goldberg F, Muradali D. Papillary lesions of the breast: MRI, ultrasound, and mammographic appearances. *AJR Am J Roentgenol* 2012; 198: 264-271. (PMID: 22268167) [\[Crossref\]](#)
- You C, Peng W, Shen X, Zhi W, Yang W, Gu Y. Solid papillary carcinoma of breast: Magnetic resonance mamography, digital mammography, and ultrasound findings. *J Comput Assist Tomogr* 2018; 42: 771-775. (PMID: 29613993) [\[Crossref\]](#)
- Nassar H, Qureshi H, Adsay NV, Visscher D. Clinicopathologic analysis of solid papillary carcinoma of the breast and associated invasive carcinomas. *Am J Surg Pathol* 2006; 30: 501-507. (PMID: 16625097) [\[Crossref\]](#)
- Zhong E, Cheng E, Goldfischer M, Hoda SA. Papillary lesions of the male breast: A study of 117 cases and brief review of the literature demonstrate a broad clinicopathologic spectrum. *Am J Surg Pathol* 2020; 44: 68-76. (PMID: 31403965) [\[Crossref\]](#)
- Karakas C, Resetkova E, Sahin AA. Papillary lesions of the breast. In: Palazzo JP, editor. *Difficult Diagnoses in Breast pathology*. Demos Medical Publishing; 2011. p. 56-87. [\[Crossref\]](#)
- Rinaldi P, Ierardi C, Costantini M, Magno S, Giuliani M, Belli P, et al. Cystic breast lesions. sonographic findings and clinical management. *J Ultrasound Med* 2010; 29: 1617-1626. (PMID: 20966473) [\[Crossref\]](#)
- Günhan-Bilgen I, Zekioglu O, Ustün EE, Memis A, Erhan Y. Invasive micropapillary carcinoma of the breast: clinical, mammographic, and sonographic findings with histopathologic correlation. *AJR Am J Roentgenol* 2002; 179: 927-931. (PMID: 12239039) [\[Crossref\]](#)
- Zekioglu O, Erhan Y, Ciris M, Bayramoglu H, Ozdemir N. Invasive micropapillary carcinoma of the breast: high incidence of lymph node metastasis with extranodal extension and its immunohistochemical profile compared with invasive ductal carcinoma. *Histopathology* 2004; 44: 18-23. (PMID: 14717664) [\[Crossref\]](#)
- Kim MJ, Gong G, Joo HJ, Ahn SH, Ro JY. Immunohistochemical and clinicopathologic characteristics of invasive ductal carcinoma of breast with micropapillary carcinoma component. *Arch Pathol Lab Med* 2005; 129: 1277-1282. (PMID: 16196516) [\[Crossref\]](#)
- Ciurea A, Calin A, Ciortea C, Ducea SM. Ultrasound in the diagnosis of papillary breast lesions. *Med Ultrasound* 2015; 17: 392-397. (PMID: 26343090) [\[Crossref\]](#)
- Speer ME, Adrada BE, Arribas EM, Hess KR, Middleton LP, Whitman GJ. Imaging of intracystic papillary carcinoma. *Curr Probl Diagn Radiol* 2019; 48: 348-352. (PMID: 30072190) [\[Crossref\]](#)
- Maluf HM, Koerner FC. Solid papillary carcinoma of the breast. A form of intraductal carcinoma with endocrine differentiation frequently associated with mucinous carcinoma. *Am J Surg Pathol* 1995; 19: 1237-1244. (PMID:7573685) [\[Crossref\]](#)
- Tsang WY, Chan JK. Endocrinal ductal carcinoma in situ (E-DCIS) of the breast: a form of low-grade DCIS with clinicopathologic and biologic characteristics. *Am J Surg Pathol* 1996; 20: 921-943. (PMID: 8712293) [\[Crossref\]](#)
- Adrada B, Arribas E, Gilcrease M, Yang WT. Invasive micropapillary carcinoma of the Breast: Mammographic, sonographic and MRI features. *AJR Am J Roentgenol* 2009; 193: 58-63. (PMID: 19542384) [\[Crossref\]](#)
- Yun SU, Choi BB, Shu KS, Kim SM, Seo YD, Lee JS, et al. Imaging findings of invasive micropapillary carcinoma of the breast. *J Breast Cancer* 2012; 15: 57-64. (PMID: 22493629) [\[Crossref\]](#)
- Dogan BE, Whitman GJ, Middleton LP, Phelps M. Intracystic papillary carcinoma of the breast. *AJR Am J Roentgenol* 2003; 181: 186. (PMID: 12818855) [\[Crossref\]](#)
- Yılmaz R, Cömert RG, Aliyev S, Toktaş Y, Önder S, Emirikçi S, et al. Encapsulated papillary carcinoma in a man with gynecomastia: ultrasonography, mammography and magnetic resonance imaging features with pathologic correlation. *Eur J Breast Health* 2018; 14: 127-131. (PMID: 29774323) [\[Crossref\]](#)
- Muttarak M, Lerttumnongtum P, Chaiwun B, Peh WCG. Spectrum of papillary lesions of breast:clinical, imaging and pathologic correlation. *AJR Am J Roentgenol* 2008; 191: 700-707. (PMID: 18716096) [\[Crossref\]](#)
- Lam WW, Chu WC, Tang AP, Tse G, Ma TK. Role of radiologic features in the management of papillary lesions of the breast. *AJR Am J Roentgenol* 2006; 186: 1322-1327. (PMID: 16632726) [\[Crossref\]](#)
- Bazzocchi M, Berra I, Francescutti GE, Del Frate C, Zuiani C, Puglisi F, et al. Papillary lesion of the breast: diagnostic imaging and contribution of percutaneous needle biopsy with 14G needle. *Radiol Med* 2001; 101: 424-431. (PMID: 11479438) [\[Crossref\]](#)
- Linda A, Zuiani C, Girometti R, Londero V, Machin P, Brondani G, et al. Unusual malignant tumors of the breast: MRI features and pathologic correlation. *Eur J Radiol* 2010; 75: 178-184. (PMID: 19446418) [\[Crossref\]](#)
- Rodríguez MC, Secades AL, Angulo JM. Best cases from the AFIP: intracystic papillary carcinoma of the breast. *Radiographics* 2010; 30: 2021-2027. (PMID: 21057133) [\[Crossref\]](#)